Engineering Journal of Qatar University, Vol. 4, 1991, p. 103 - 120.

SOLIDIFICATION OF STEEL BILLETS IN CONTINUOUS CASTING

A. Y. Kandeil*, I. A. Tag* and M. A. Hassab**
* Mechanical Engineering Department, Qatar University
Doha, Qatar, Arabian Gulf
** Faculty of Engineering, Alexandria University, Alexandria, Egypt.

ABSTRACT

For practical operation, it is necessary to know how the solidification of liquid steel progresses i.e. when and where a strand has completely solidified. Decisions on, the casting speed, the spray water flow rates and super-heating in the tundish can only be made with the knowledge of the solidification progress.

This paper describes the theoretical phenomena of the cooling inside the mould and in the secondary cooling zone. To achieve this a mathematical unsteady, two dimensional heat conduction model has been developed for computing the temperature field and to study the effect of casting parameters on the metallurgical properties during bar solidification. The predicted solidified thickness profile in the mould region was compared with the measured profile and good agreement has been established.

NOMENCLATURE

C	:	specific heat of solidifications defined by $C = C_P + H_s/(T_L - T_S)$	kJ/kg C
Cp	:	specific heat of steel	kJ/kg C
H	:	water-spray heat transfer coefficient	kW/M² C
H_s	:	latent heat of solidification	kJ/kg
L_s	:	distance required for complete solidification	m
q_s	:	heat flux at mould-strand interface	kW/m²
T	:	temperature	°C
u	:	casting speed	m/min
T_L	:	liquidus temperature	°C
T_s	:	solidus temperature	°C
T_{sa}	:	average surface temperature	°C
t	:	time	min
x,y	:	horizontal coordinates	m
X_s	:	thickness of solid layer	mm
z	:	direction of casting	
W_1, W_2	:	width and depth of billet	m
α	:	thermal diffusivity	m²/s
ρ	:	density of steel	kg/m³

INTRODUCTION

This paper presents results on mathematical modelling and solidification of steel billets during the continuous casting process. The continuous casting process, which is the preferred route for converting liquid steel to semi-finished shapes, has attained a high degree of sophistication in comparison to many other metallurgical operations. This advanced state of development can be attributed, in part, to the extensive application of mathematical models in combination with valid in plant measurements. The models have contributed to our fundamental understanding of the process which then led to improvements in the design and operation. The measurements, although difficult, have been vital to the success of the modelling effort as they have been needed to characterize boundary conditions and to validate model predictions.

In the continuous casting process of steel billets shown schematically in Figure (1), molten steel is poured from a refractory tundish into a water-cooled copper mould. The semi-solidified steel strand is withdrawn with a constant speed, cooled by water sprays in both the submould region and the secondary region until solidification is complete [1]. For practical operation it is necessary to know how the solidification of liquid steel progresses, i.e. when and where a strand has completely solidified. Decisions on, for example, the casting speed or the spray water flow rates can only be made with the knowledge of the solidification progress. Good quality and high productivity are required in continuous casting. In

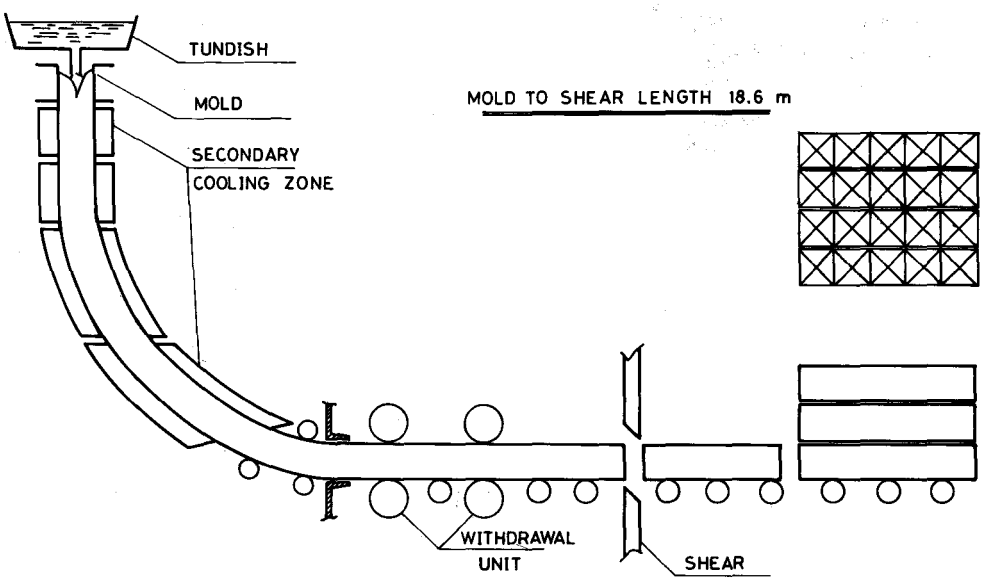

Fig. 1: Schematic of continuous casting machine

practice, they are both determined by heat transfer and the stress status of billet solidification. For example, the metallurgical standards of solidification, such as the solidified thickness at the exit of the mould, the liquid pool depth, and the slab surface temperature, are governed by heat transfer characteristics. Therefore, we must select suitable parameters if we are to obtain the metallurgical criterion of good quality steel bars.

METALLURGICAL REQUIREMENTS OF BAR SOLIDIFICATION

In order to achieve high productivity and good quality bars, we must ensure that the casting machines are running smoothly. Technologically, the metallurgical standards of bar solidification should be as follows [2]:

1. The solidification shell at the exit of the mould should be thick enough to avoid breakouts, while maintaining a high casting speed.

2. During bar solidification, which normally occurs throughout the liquid pool depth, deformation should be confined within certain limits.

3. Deformation capacity of the solidified crust should be limited. From a high temperature brittleness curve [3], it can be seen that 700-750 C corresponds to the lowest elasticity, and at 900-1100 C the elasticity is at its highest value. A bar of an average surface temperature of over 900 C before straightening is ideal, according to steel grade.

4. Bulging limits of the bar crust should be observed. Due to ferro-static pressure of the liquid steel, bulging may occur between the two rollers, creating tensile stresses along the solidification front, and causing a central segregation line.

Considerable research has been conducted in the mathematical modelling of continuously cast slab solidification [4-6]. The results obtained from the models, that are based on a one-dimensional, unsteady-state heat conduction equation, furnish the relationship between the metallurgical standards required by the process and slab quality. They also lead to practical improvements in the control of slab solidification.

Two dimensional heat transfer mathematical models of the continuous casting in the primary zone, have been developed. These models predict the temperature field and profile in the solidified steel bars in order to estimate the optimal casting conditions for such process [7-12]. In these simulations the problem arised from the formation of the air gap between the cooled strand and the mould due to the shrinkage of the former has been dealt with in several ways. Other investigators [8-10] have used estimated values for the heat transfer coefficients to calculate the temperature distribution in the casting. Researchers [7,9] have used experimentally

measured heat flux data obtained on the water side of the casting model. In some analysis [11, 12] the air gap was calculated by combining thermal and stress analysis. The possible deformation of the continuous casting mould was not considered. Samarasekera and Brimacombe [12] have shown that mould deformation has a significant influence on the gap thickness and therefore the casting heat transfer. The objective of this study is to develop a mathematical model for a continuously cast billet solidification capable of analyzing various aspects of the process, and hence optimizing operating conditions.

MATHEMATICAL MODEL

A two-dimensional, unsteady state heat flow model based on the ADI finite difference method, has been developed to predict the temperature field and shell profile in the solidified steel strand for the submould and secondary regions. A schematic of the problem is shown in Fig. 2. In the model, the following assumptions were made:

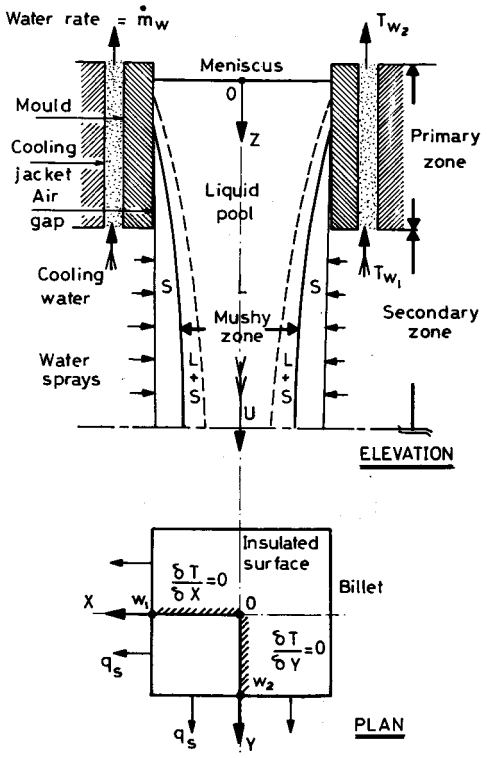

Fig. 2: Illustration of sectional geometry in the continuous casting zones

1. Conduction in the longitudinal direction of the billet has been neglected, since longitudinal temperature gradient is much less than transverse gradient.
2. Convection heat transfer in the liquid pool was neglected (an assumption justified by Mizikar *et al.* [5]) and only conductive flow is considered.
3. The latent heat of fusion evolved during solidification is taken into account by adjusting the specific heat over the range of solidification $C = cp + H_s/(T_L - T_S)$.
4. The cast is symmetrical relative to its center planes and only one quarter of the cross-section was modeled.
5. The surface heat flux was based on the experimental measurements of the shell profile of the solid region in the submould region and data obtained on the water side of the casting mould. The surface heat flux was assumed to vary in the longitudinal direction.
6. The interface resistance between the strand and mould was neglected by considering a tapered mould to prevent the formation of air gap.
7. The steel billet in the secondary zone was considered cooled by water sprays. Heat is dissipated from its outer surface via convection.
8. The convective heat transfer coefficient in the secondary zone which is a function of spray water flow rate is considered as a parameter that covering a wide range of water rates.

Under these assumptions the model is completely described by the following equations:

Conduction Equation:

$$\rho C \frac{\partial T}{\partial t} = \frac{\partial}{\partial x}\left(k \frac{\partial T}{\partial x}\right) + \frac{\partial}{\partial y}\left(k \frac{\partial T}{\partial y}\right) \tag{1}$$

Boundary and Initial conditions:

$$\frac{\partial T}{\partial x} = 0 \qquad x = 0 \tag{2}$$

$$-k \frac{\partial T}{\partial x} = q_s(t) \qquad x = \frac{X_1}{d} \tag{3}$$

$$\frac{\partial T}{\partial y} = 0 \qquad y = 0 \tag{4}$$

$$-k\frac{\partial T}{\partial y} = q_s(t) \qquad y = \frac{Y_1}{2} \tag{5}$$

$$T(x,y) = T_p \qquad t = 0 \tag{6}$$

$$C = \begin{cases} C_p & T > T_L \text{ or } T < T_s \\ C_p + \dfrac{H_s}{T_L - T_s} & T_s < T < T_L \end{cases} \tag{7}$$

and q_s = surface heat flux to be determined based on experimental measurements. X_1 and Y_1 are length and width of the transverse plane of the bar which is considered as square.

For a uniform casting speed throughout the entire region of the steel bar the relation between the longitudinal direction z and the time t for a slice of steel to move a distance z in casting machine becomes,

$$z = u \,.\, t \tag{8}$$

under this condition, equation (1) transforms to the following form:

$$\rho\, Cu\frac{\partial T}{\partial z} = \frac{\partial}{\partial x}\left(k\frac{\partial T}{\partial x}\right) + \frac{\partial}{\partial y}\left(k\frac{\partial T}{\partial y}\right) \tag{9}$$

Subject to:

$$\frac{\partial T}{\partial x} = \qquad x = 0 \tag{10}$$

$$-k\frac{\partial T}{\partial x} = q_s(z) \qquad x = \frac{W_1}{2} \tag{11}$$

$$\frac{\partial T}{\partial y} = 0 \qquad y = 0 \tag{12}$$

$$-k\frac{\partial T}{\partial y} = q_s(z) \qquad y = \frac{W_2}{2} \tag{13}$$

$$T(x,y) = T_p \qquad z = 0 \tag{14}$$

MODEL SOLUTION

The system of equations (9) to (14) is solved numerically using the Alternating Direction Implicit method (ADI) to analyze the effect of the technological

parameters on bar solidifications. This method has the advantage that guarantee stability. In this method, the square cross-section of the bar is divided into N x N square meshes of size $\Delta x * \Delta x$ (i.e. $\Delta y = \Delta x$). Finite difference approximation carried out on equation (9) can be presented as:

$$\rho C_p \left(\frac{T^{n+1}_{i,j} - T^{n}_{i,j}}{\Delta t}\right) = k\left(\frac{T^{p}_{i-1,j} - 2T^{p}_{i,j} + T^{p}_{i+1,j}}{\Delta x^2}\right) + k\left(\frac{T^{q}_{i,j-1} - 2T^{q}_{i,j} + T^{q}_{i,j+1}}{\Delta y^2}\right) \tag{15}$$

where the integers p and q are alternating their values from a time increment to another as follows:

$n = 1,3,5,7,\ldots\ldots$ $(\rho = n+1,\ q = n)$,
and
$n = 2,4,6,8,\ldots\ldots$ $(\rho = n,\ q = n+1)$

$(x = (i-1)\Delta x,\ y = (j-1)\Delta y,\ t = n\Delta t)$

under this assumption, the above equation has two different forms for every two time steps. They can be given in the following forms:

Case of n = 1,3,5,.....

$$a_{i,j}\, T_{i-j} + b_{i,j}\, T_{i,j} + C_{i,j}\, T_{i+1,j} = d_{i,j} \tag{16}$$

Case of n = 2,4,6,8,.....

$$a_{i,j}\, T_{i,j-1} + b_{i,j}\, T_{i,j} + c_{i,j}\, T_{i,j+1} = d_{i,j} \tag{17}$$

$a_{i,j} = c_{i,j} = R_{i,j}$

$b_{i,j} = -(1+2\ R_{i,j})$

$d_{i,j} = \{ - T^{0}_{i,j} - R_{i,j}\ (T^{0}_{i,j-1} - 2T^{0}_{i,j} + T^{0}_{i,j+1})$ $(n=1,3,5,..)$

$= - T_{i,j} - R_{i,j}\ (T^{0}_{i-1,j} - 2T^{0}_{i,j} + T^{0}_{i+1,j})$ $(n=2,4,6,..)$

$R_{i,j} = (\alpha\ \Delta t/\Delta x^2)$

$\alpha = k/\rho\ C_p$

The superscript 'o' refers to previous time $(t=n\Delta t)$ and the terms without superscript refer to present time $t = (n+1)\ \Delta t$. Each one of equations (16) & (17) contains six temperature terms, only three of them (at t = n t) are known. They constitute a tridiagonal set of simultaneous equations. The finite difference equations at the boundary surfaces and corners can be obtained from equations (10) to (14), the resultant expressions together with equations (16) and (17) for the interior points constitute a system of linear square matrix of order NxN. This

system can be solved numerically using the conventional Guess-Jordan elimination technique to get the temperature field at different times.

In our computations, the following reference parameters taken from QASCO (base case) are considered:

Mould dimension:

Cross-section	:	150 x 150	mm
Height	:	80	mm
Meniscus level	:	120	mm
Billet length from mould to shear	:	18.6	m
Mould water temperature:			
Inlet	:	21.1	^{0}C
Outlet	:	31.1	^{0}C
Mould water flow rate	:	80	m^3/hr
Casting speed	:	1.8	m/min
Molten steel temp. at meniscus level	:	1540	^{0}C
Steel composition	:	C=0.38%	Si=0.16%
		Mn=1.33%,	S=0.013%
Liquidus temperature	:	1500	^{0}C
Solidus temperature	:	1465	^{0}C
Heat transfer coefficient between water and billet in secondary zone	:	3	kw/m^2 ^{0}C

DISCUSSION

The steel-to-mould heat flux is an extremely important controlling factor in the process of continuous casting. Heat flux is a maximum at the meniscus and declines to about one-fourth this value at the mould exit. This variation arises because heat transfer between steel and mould is governed primarily by conduction across the gap separating the two solids, and the gap is smallest at the meniscus.

Brimacombe and his colleagues, predicted the axial mould heat flux distribution through an iterative procedure using different steel-to-mould heat fluxes until a match was obtained between measured and predicted temperatures. In their industrial trials, the mould was instrumented with intrinsic copper-constantan thermocouples, a procedure which was considered with costly and laborious.

In our work, based on Brimacombe findings, and on the in-house developed one-dimensional continuous casting mathematical model, the growth of the solid shell was either under-estimated or over-estimated when compared with the measured experimental values. Modifications accomplished to the existing heat flux models presented by Brimacombe through changing the ratio of the heat flux

at the meniscus to that at the exit, did not give the anticipated agreement, Figure (3).

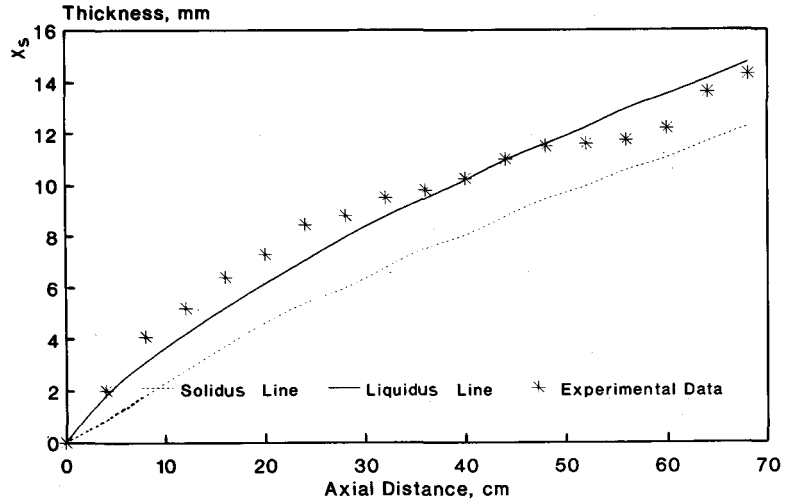

Fig. 3: Solidification profile in primary cooling zone for $q_s = 2680 - 335\ (Z/U)^{**}$ 0.5 KW/m^2

To check the validity of our model, a new correlation for heat flux based on QASCO profile measurements is developed. Using this correlation, it is evident that the agreement between measured and predicted profiles is good at both the top and the bottom of the strand, Figure (4).

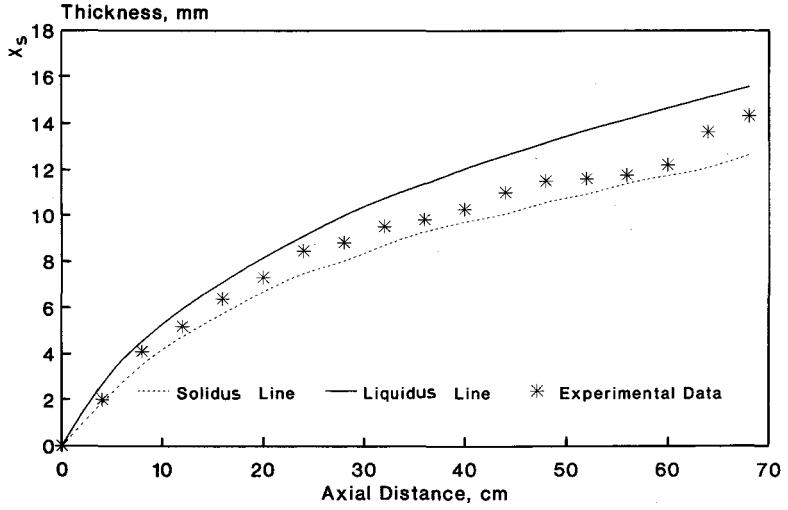

Fig. 4: Solidification profile in primary cooling zone for $q_s = 2275^* [2.6 - 6.9\ (Z/L) + 5.6\ (Z/L)^{**} 2]$

To check the adequacy of using the simple one dimensional model used by several investigators, the thickness of the solidified layer predicted by the one-dimensional (1-D) an two-dimensional (2-D) models were presented and compared with the experimental results.

Calculations were performed on QASCO steel for the growth of the solidified layer at the mid span of one of the strand's sides. Experimental measurements were performed on a strand taken during break out. Details of the mould and location of break out are shown in Figure (5). The strand was sectioned, Figure (6) at both the longitudinal and transverse directions and thickness profiles were determined.

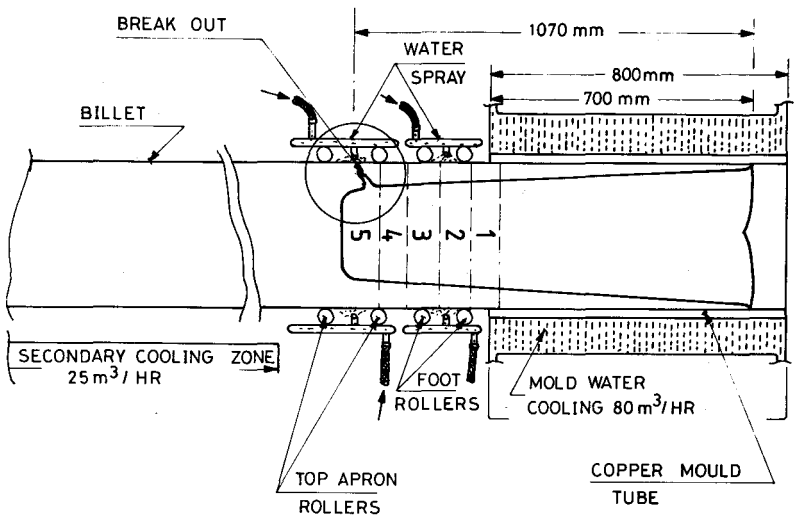

Fig. 5: Schematic showing details of primary cooling zone and location of break out

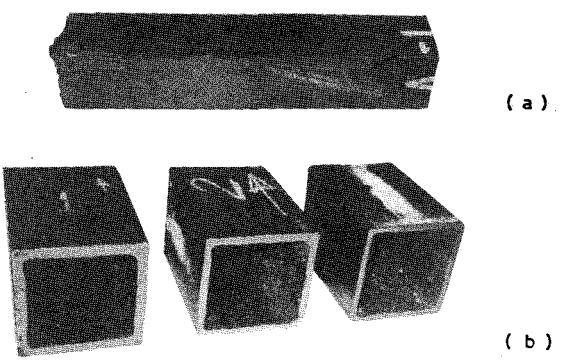

Fig. 6: Continuous casting slab obtained from primary cooling zone during interrupted run. (a) Complete piece. (b) Sections showing thickness profile

Solidification rate in primary zone based on the one-dimensional and the two-dimensional models is presented in Figure (7) for different casting speeds. It can be seen that at the mid-span the 1-D model accurately predicts the shell growth in the primary region; where the effect of the corners is not yet significant. As expected, solidified thickness decreases with casting speed. At higher casting speeds, contact between mould and strand takes a shorter time with reduction in heat transfer from the strand.

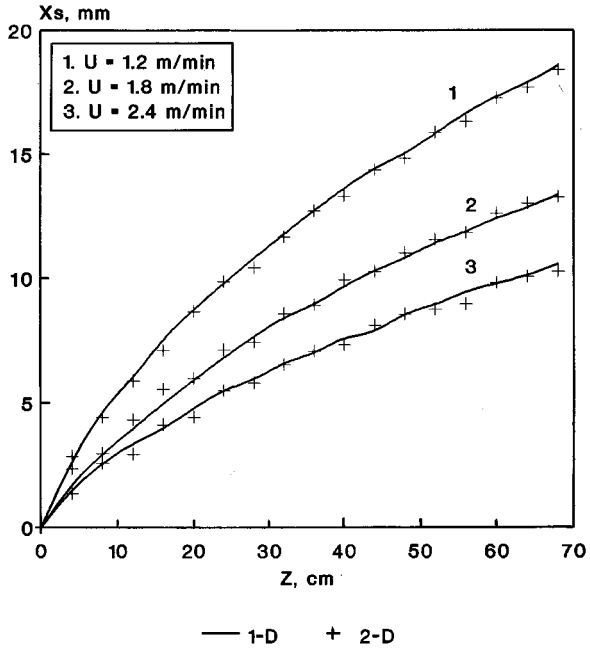

Fig. 7: Solidification rate in primary zone based on 1-D & 2-D models

Figure (8) shows the effect of casting speed, within the range considered, on the shell thickness at the exit of the mould as predicted from the 1-D model. The 1-D model, however, cannot be used in the secondary zone where corner effects are significant, as verified from the measured data. Therefore the following results will be based on the 2-D model.

The effect of casting speed on the solidification rate in the secondary cooling zone, of infinite length, is illustrated in Figures (9) to (11). These figures present the isothermal contours of the liquidus and solidus temperatures (1500 ^{0}C & 1465 ^{0}C) at various distances down the strand for the accepted range of casting speeds (1.2, 1.8 & 2.4 m/min). As shown in Figure (12), the increase of casting speed from 1.2 m/min to 2.4 m/min causes a linear increase in the solidified length from 5.07 to

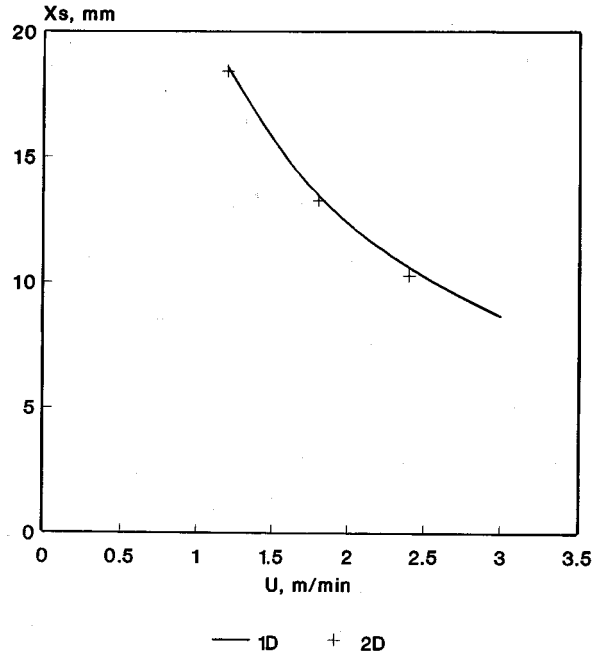

Fig. 8: Casting speed Vs shell thickness at the exit of primary zone

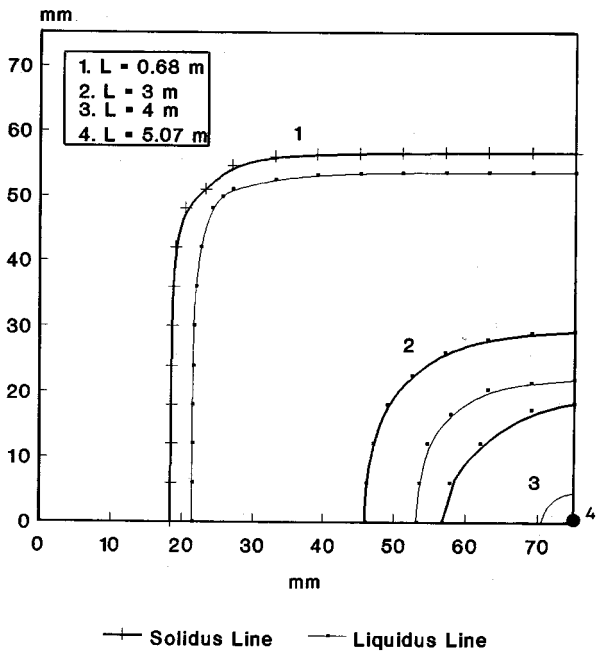

Fig. 9: Progress of solidus and liquidus contours for U = 1.2 m/min

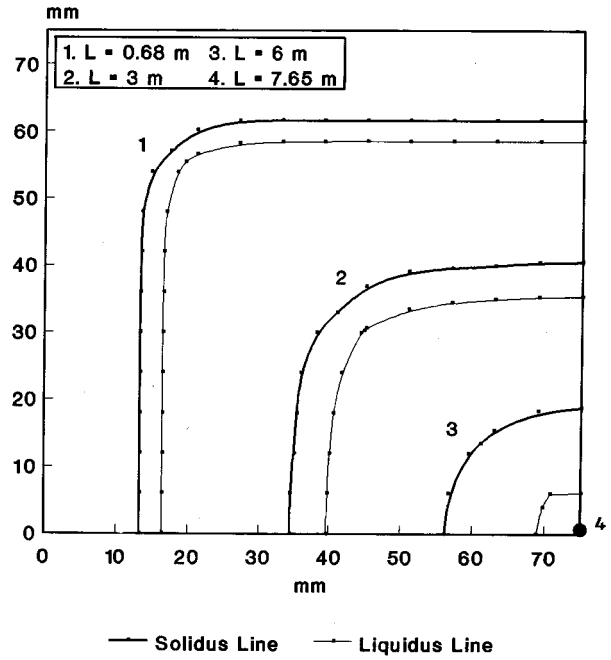

Fig. 10: Progress of solidus and liquidus contours for U = 1.8 m/min

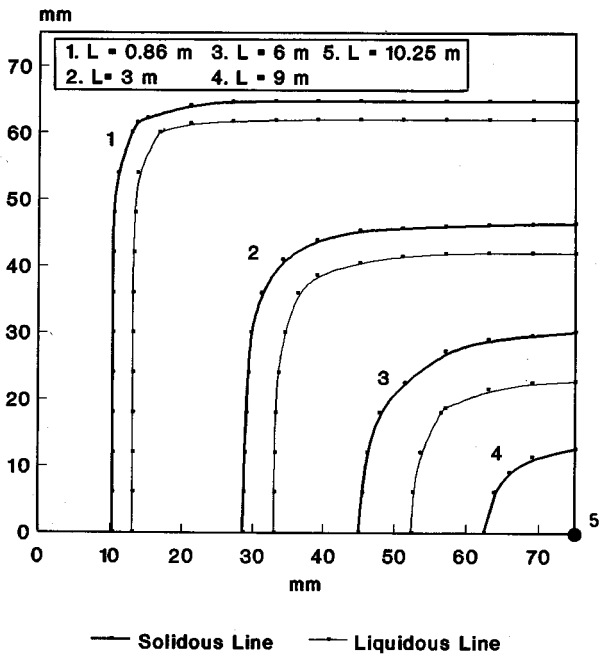

Fig. 11: Progress of solidus and liquidus contours for U = 2.4 m/min

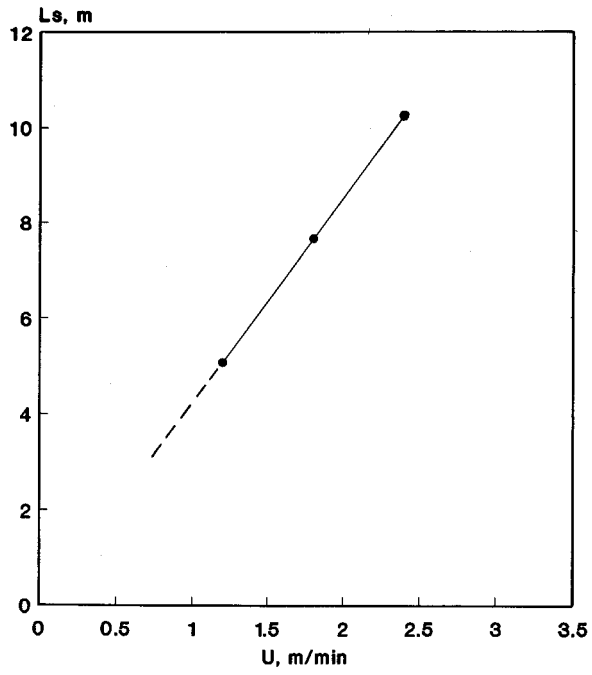

Fig. 12: Effect of casting speed on distance needed for complete solidification (t_s = slope = 4.25 min.)

10.15m. This gives an indication that cooling time is the same for all cases considered, i.e. independent of casting speed. Total cooling time needed for completely solidifying the liquid steel is 4.25 min with about 10% of this time being spent in the primary zone. Figure (13) shows solidification progress with casting speed.

Although casting speed affects solidification rate of strand in primary zone, the short length of the zone compared with that of the secondary zone renders that effect negligible on the total cooling time. Moreover, the surface cooling in the secondary zone is due to the use of high speed water flow from spray nozzles, i.e. forced convection cooling. The thickness of mushy zone — bounded by liquidus and solidus contours, is getting thicker as distance (proportional to speed) increases, as shown earlier in Figure (4). This increase in thickness is due to the increase in the thermal resistance of the continuously grown solid region. Thus the solidification rate will slow down at the expense of cooling the solid layer, as cooling continues until maximum temperature at the center of strand approaches the solidus temperature.

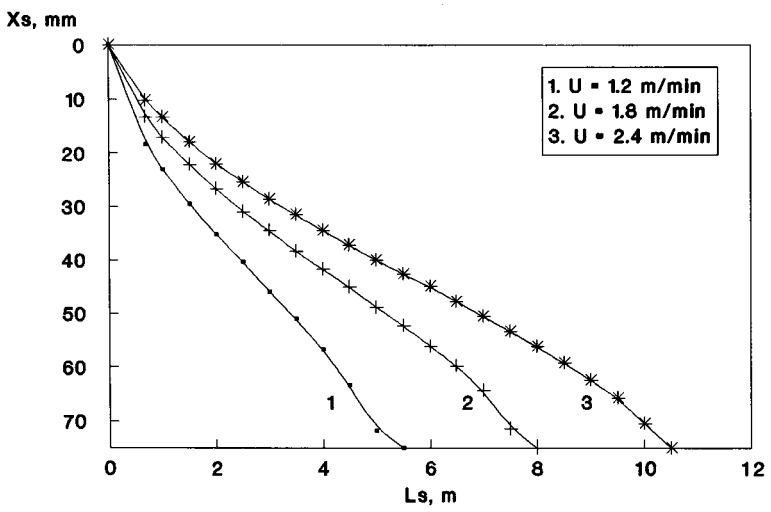

Fig. 13: Effect of casting speed on solidification progress

The effect of water spray intensity for a specific nozzle arrangement expressed by spray water-related heat transfer coefficient H, on the average surface temperature of the billet is shown in Figures (14) and (15). The surface temperature of strands can influence steel quality, i.e. by causing surface and internal cracks. Steel should be kept at a surface temperature near 800 ^{0}C during bending to avoid cracking. Therefore, knowledge of water cooling parameters affecting surface temperature is of much concern. Values of temperatures shown in Figure (14) indicate that water

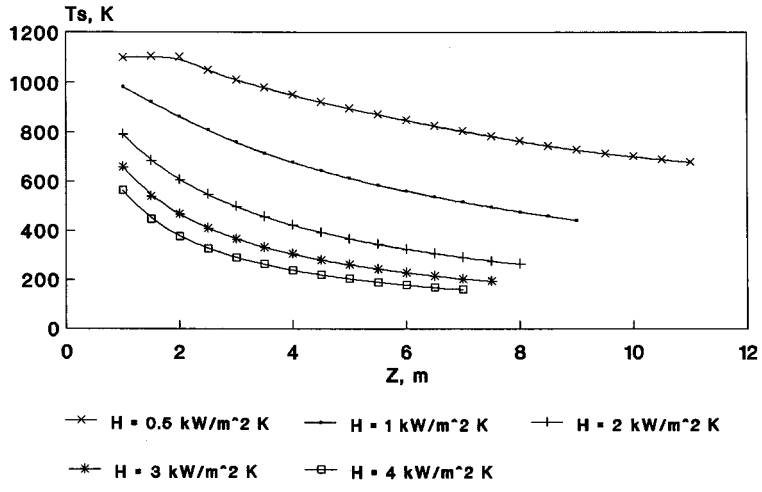

Fig. 14: Average surface temperature V_s water-spray heat transfer coefficient

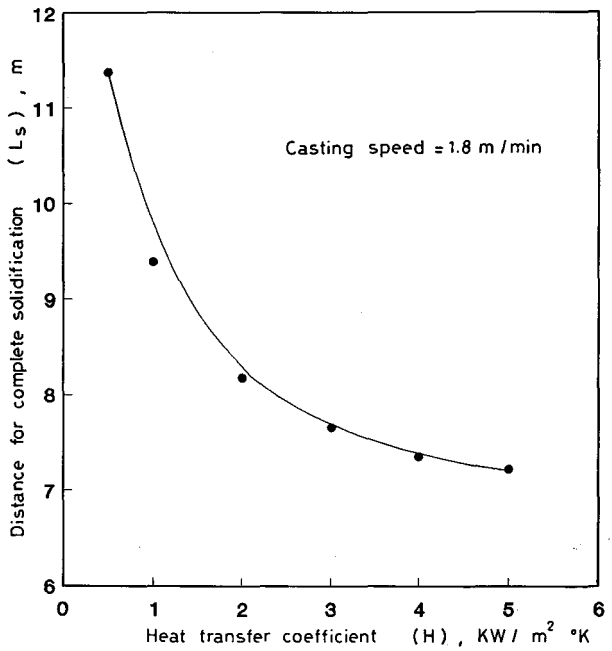

Fig. 15: Effect of water-spray heat transfer coefficient on distance needed for complete solidification

cooling rate should be kept at its lowest acceptable level to keep these temperatures near the recommended values.

It is also noted that averag surface temperature of the billet is always higher than the minimum acceptable value (800 ^{0}C), even under the lowest water-surface cooling condition. To achieve such a temperature, water cooling should be followed by air cooling of much lower rate before bending of the strand starts. Minimum average surface temperature reached at the end of solidification is about 680 ^{0}C. Further air cooling from the surrounding will cause a rise in surface temperature in spite of the drop in body temperature. The reason for this is that, cooling by water causes higher rate of surface cooling, and sharp drop in temperature in the layer near the surface. Switching to air cooling — a bad conductor — causes drop in the surface heat flux with a subsequent increase in surface temperature.

Figure (15) shows the effect of water cooling rate on distance needed for complete solidification L_s for U = 1.8 m/min. Higher surface cooling rates, lead to shorter cooling times and shorter distances. Thus, total cooling time is mainly affected by surface cooling either directly as in the secondary zone, or indirectly as in the primary zone. However the largest L_s = 11.37 m corresponding to the lowest

heat transfer coefficient, and the lowest water spray intensity, is still much shorter than the presently used length = 18.6 m. The difference in length allows an increase in the surface temperature reaching the desired value.

CONCLUSION

A two dimensional mathematical model for computing temperature field in a solidifying continuously cast billets under specified parameters is presented in this report. The model accounts for the technological standard adopted in industrial practice. Parameters considered are: surface heat flux, casting speed and heat transfer coefficient in the secondary zone.

The predicted results concerning solidification rate in the primary zone are found in good agreement with the experimental ones. The model allows the understanding of the relationship between casting parameters and technological standards required for better steel quality and efficient casting process.

REFERENCES

1. **Birt, J.P.** *et al.* 1979, Rev. Metall., Paris, p. 29.

2. **Brimacombe, J.K., Samarasekera, I.V.** and **Bommaraju, R. 1986,** Proceedings of the Fifth International Iron and Steel Congress in Washington, D.C., p. 409-423.

3. **Cai, K.** and **Liu, P. 1984,** Control of solidification process during continuous casting of steel, Acta Metall. Sin. (China), Vol. 20 (3) B146-B154.

4. **Clyne, T.W.** and **Garcia, A. 1980,** Assessment of a new model for heat flow during unidirectional solidification of metals, Int. J. Heat Mass Transfer, Vol. 23, p. 773-782.

5. **Grill, A., Sorimachi K.** and **Brimacombe, J.K. 1976,** Metall. Trans., Vol. 7B, No. 2, p. 177.

6. **Hills, A.W.D. 1969,** TMS/AIME, 245, p. 1471-1479.

7. **Lait, J.E. 1974,** *et al.*, Ironmaking & Steelmaking, Vol. 1 (2), p. 90.

8. **Mizikar, E.A. 1967,** Trans. Metall. Soc. AIME, Vol. 239, p. 1747-1753.

9. **Perkins, A.** and **Irving, W.R. 1975,** Math. Process Models in Iron and Steelmaking, The Metals Soc., London, p. 187.

10. **Samarasekera, I.V.** and **Brimacombe, J.K. 1979,** Can. Met. Quart., Vol. 18, p. 251.